GMR
The Original

STARCH/PVA ELECTROSPUN NANOSCAFFOLDS INCORPORATED WITH ULTRASONIC-ASSISTED GREEN SYNTHESIS OF CuO NANOPARTICLES FROM, A BROWN MARINE MACROALGAE (*Sargassum wightii*) EXTRACT: *IN VITRO* WOUND HEALING ANALYSIS

Karneesh Kumar[1], Chakradhar Arepalli[2], Sattanathan Govindharajan[3]*

[1]Saveetha Medical College & Hospital (SMCH), Saveetha Institute of Medical and Technical Sciences (SIMATS), Thandalam, Chennai, Tamil Nadu 602105, India. kkarneesh8@gmail.com
[2]Department of Nephrology, Saveetha Medical College and Hospital, Saveetha Institute of Medical And Technical Sciences (SIMATS), Thandalam, Chennai-602105, Tamil Nadu, India. Email: arepalli.chakri@gmail.com
[3]Department of Pathology, Saveetha Medical College and Hospital, Saveetha Institute of Medical And Technical Sciences (SIMATS), Thandalam, Chennai-602105, Tamil Nadu, India. Email: sattanathanphd@gmail.com
*Corresponding Author: sattanathanphd@gmail.com (S.G.)

ABSTRACT

This study explores the development and characterization of starch/polyvinyl alcohol (PVA) electrospun nanoscaffolds incorporated with copper oxide nanoparticles (CuO NPs) synthesized via an ultrasonic-assisted green method using *Sargassum wightii* extract. The phytochemical-rich algal extract facilitated the eco-friendly synthesis of CuO NPs, confirmed by UV-Visible spectroscopy with a characteristic surface plasmon resonance (SPR) peak at 292 nm. Fourier-transform infrared (FTIR) spectroscopy revealed functional groups involved in nanoparticle stabilization and polymer interactions, while X-ray diffraction (XRD) confirmed the monoclinic crystalline structure of CuO NPs. Scanning electron microscopy (SEM) demonstrated uniform nanoparticle distribution within the nanofibrous scaffold, which exhibited a porous and bead-free morphology conducive to cell attachment. Thermogravimetric analysis (TGA) indicated thermal stability up to 220°C, and dynamic light scattering (DLS) measurements showed colloidal stability with a zeta potential of −12 mV. The wound healing potential was evaluated using an *in vitro* scratch assay on HaCaT keratinocytes. The starch/PVA/CuO-NPs nanoscaffolds exhibited superior wound closure (48.62–96.62%) compared to standalone CuO NPs (41.62–84.62%) and algal extract (33.62–70.62%), highlighting their synergistic efficacy. These findings suggest that the composite nanoscaffolds enhance cell migration and proliferation, making them a promising candidate for wound healing applications. The study underscores the potential of green-synthesized CuO NPs and biopolymer nanoscaffolds in regenerative medicine.

KEYWORDS: *Sargassum wightii*, Green synthesis, CuO NPs, Starch/PVA/CuO-NPs nanoscaffolds, Wound-healing activity.

1. INTRODUCTION

The skin, as the body's largest organ, plays a pivotal role in safeguarding internal tissues from external pathogens, regulating temperature, and facilitating sensory reception [1]. However, when this protective barrier is compromised due to injuries such as cuts, burns, or surgical incisions, it necessitates prompt and efficient wound healing [2]. The natural wound healing process involves a complex interplay of cellular and molecular events—namely hemostasis, inflammation, proliferation, and tissue remodeling [3]. While this process is remarkably effective under normal physiological conditions, several factors like infection, diabetes, and aging can delay or impair healing [4]. To address these limitations, the development of bioengineered wound dressings has become a focal point in modern biomedical research, particularly those that can support tissue regeneration while offering antibacterial protection [5].

In recent years, electrospun nanofibrous scaffolds have emerged as highly promising materials for wound healing applications due to their unique structural and functional properties [6]. Mimicking the extracellular matrix (ECM), these scaffolds provide a conducive microenvironment for cellular adhesion, migration, and proliferation [7]. Among the various polymers used in scaffold fabrication, starch and polyvinyl alcohol (PVA) have garnered considerable attention owing to their biocompatibility, biodegradability, and film-forming abilities [8]. Starch, a natural polysaccharide, offers excellent moisture retention and non-toxicity, whereas PVA enhances the mechanical integrity and hydrophilicity of the resulting composite material [8]. The synergy between these two polymers enables the fabrication of flexible, porous, and robust nanofibers ideal for wound management [9].

The functionality of wound dressing materials can be further enhanced by incorporating nanoparticles, particularly metal oxides such as copper oxide nanoparticles (CuO NPs), which exhibit strong antimicrobial, anti-

inflammatory, and angiogenic properties [10]. CuO NPs have been shown to accelerate wound closure by promoting fibroblast proliferation, collagen deposition, and neovascularization [11]. However, conventional chemical synthesis methods for CuO NPs often involve toxic reagents and harsh reaction conditions that can hinder their biomedical applicability [12]. To overcome these drawbacks, green synthesis strategies utilizing biological sources, including plants, algae, and microorganisms, have emerged as environmentally sustainable and biocompatible alternatives [13].

Marine macroalgae, especially brown algae such as *Sargassum wightii*, are rich in diverse bioactive compounds including polyphenols, flavonoids, terpenoids, and polysaccharides [14]. These phytochemicals can act as natural reducing and stabilizing agents during nanoparticle synthesis, making them ideal candidates for green nanotechnology [15]. *S. wightii* is abundantly available along the coastal regions of Tamil Nadu, India, and has been traditionally used for its medicinal and nutritional value [16]. The incorporation of algal-derived CuO NPs into nanofibrous scaffolds combines the advantages of marine biotechnology and polymer science, potentially yielding advanced wound dressings with enhanced healing efficacy [17].

In this context, ultrasonic-assisted extraction methods offer a novel and efficient approach to obtaining algal extracts enriched with functional phytoconstituents [18]. Ultrasonication enhances mass transfer, breaks down cellular matrices, and releases intracellular contents without degrading sensitive compounds [19]. When coupled with green nanoparticle synthesis, this technique offers a rapid, reproducible, and eco-friendly route to fabricate functional nanomaterials [20]. Moreover, ultrasonic processing reduces reaction time and energy consumption compared to traditional heating or reflux methods, aligning with the principles of green chemistry and sustainability [21].

This research work is centered on the fabrication and *in vitro* evaluation of starch/PVA electrospun nanoscaffolds incorporated with CuO NPs synthesized via ultrasonic-assisted green synthesis using *S. wightii* extract [22]. The study explores the integration of bioactive nanoparticles within a biopolymeric scaffold to develop a multifunctional wound dressing material [23]. The CuO NPs were synthesized by reacting copper sulfate with the aqueous algal extract under controlled sonication conditions [24]. The resultant nanoparticles were characterized using advanced spectroscopic and microscopic techniques to confirm their physicochemical attributes such as particle size, surface charge, and crystallinity [25].

Subsequently, the CuO NPs were uniformly incorporated into a starch/PVA matrix to fabricate electrospun nanoscaffolds using an optimized set of electrospinning parameters [22]. The structural morphology, fiber diameter, thermal stability, and molecular interactions within the nanofibrous mats were assessed through Scanning electron microscopy (SEM), Fourier-transform infrared spectroscopy (FTIR), X-ray diffraction (XRD), Thermogravimetric analysis (TGA), and UV–Vis analyses [26]. The presence of CuO NPs within the fibrous matrix was further validated through zeta potential and dynamic light scattering (DLS) studies [27].

To evaluate the biological efficacy of the developed nanoscaffolds, an *in vitro* scratch wound healing assay was performed using HaCaT keratinocyte cells [28]. This model is widely accepted for mimicking the re-epithelialization phase of wound healing, particularly cell migration and proliferation [29]. The extent of wound closure was quantified at different concentrations of the test samples—algal extract, CuO NPs, and starch/PVA/CuO-NPs nanoscaffolds—over 24 and 48 hours [30]. The cytocompatibility and pro-migratory potential of the scaffolds were statistically analyzed to establish their wound healing effectiveness [31].

The integration of green-synthesized CuO NPs into a biopolymer-based electrospun scaffold represents a promising therapeutic platform for wound management [32]. This study contributes to the growing body of research that seeks to combine natural resources, nanotechnology, and advanced fabrication techniques for biomedical applications [33]. The approach not only offers a sustainable alternative to synthetic wound dressings but also leverages the therapeutic benefits of marine bioresources [34]. Overall, this research aims to bridge the gap between eco-friendly nanoparticle synthesis and practical wound care solutions, advancing the development of next-generation wound healing materials.

2. MATERIALS AND METHODS

2.1. Materials

This investigation employed *S. wightii*, a brown seaweed species gathered from the marine region surrounding Rameswaram, Tamil Nadu, India, as a green reductant for producing CuO NPs. Copper(II) sulfate pentahydrate ($CuSO_4 \cdot 5H_2O$), acquired from Sigma-Aldrich, was the metal precursor. PVA, with an estimated molecular weight of 115,000, was utilized as the primary electrospinnable polymer. Food-grade starch was incorporated to enhance scaffold stability. All reagents, including Milli-Q grade water and ethanol, were of analytical purity and sourced from Merck and Sigma-Aldrich. Electrospinning was executed using a HOLMARC HO-NFES-040 setup integrated with a syringe pump. Nanoparticles and scaffolds were analyzed using UV-Vis (VIS SPEC V-730), FTIR (PerkinElmer Spectrum Two), XRD (Bruker D8 Advance), SEM (JSM-IT800 NANO), DLS and zeta potential (Malvern Zetasizer Ultra), and TGA (PerkinElmer TGA 8000). Wound healing studies followed standardized validated protocols.

2.2. Collection of marine macroalgae

Fresh specimens of *S. wightii* were hand-collected from shallow marine waters near Rameswaram. The samples were thoroughly washed with tap water to eliminate sand particles, microalgae, and organic contaminants,

followed by several rinses with distilled water for further purification. Roughly 100 grams of clean algal material was chopped into small pieces and left to dry under ambient conditions for two weeks. After drying, the biomass was finely powdered using a mechanical blender and stored in airtight containers at room temperature in a moisture-free environment for subsequent use.

2.3. Ultrasonic-assisted extraction

To extract bioactive compounds, 2 g of powdered *S. wightii* was suspended in 50 mL of Milli-Q water in a 100 mL beaker. The mixture was treated using a LABQUEST ultrasonic cleaner (Borosil; Serial No. 941032329018) at 60°C for a duration of 45 minutes. Following ultrasonication, the mixture was filtered using Whatman No. 1 filter paper under aseptic conditions. The clear filtrate was collected and maintained at 10°C. For extended storage and subsequent applications, the extract was lyophilized to obtain a powdered form using a freeze-drying system [35, 36].

2.4. Green synthesis of CuO NPs

CuO NPs were generated through an eco-friendly synthesis using the aqueous extract of *S. wightii*. A solution of 0.1 M $CuSO_4 \cdot 5H_2O$ (50 mL) was blended with 10 mL of algal extract prepared from 10 mg of algal powder in Milli-Q water at a 5:1 volume ratio. The blend was stirred continuously at 650 rpm and heated to 60°C for 2 hours. A distinct color transition from blue to bluish-green indicated nanoparticle development. The reaction mixture was centrifuged and rinsed three times with deionized water to remove excess reagents. The purified nanoparticles were then freeze-dried for 48 hours and kept in powdered form for analysis and scaffold loading [37].

2.5. Fabrication of CuO-loaded electrospun starch/PVA scaffolds

A 15% (w/w) aqueous PVA solution was created by dissolving the polymer in Milli-Q water with constant stirring. Subsequently, 100 mg each of starch and CuO NPs were added and mixed at 50°C for 2.5 hours to ensure even dispersion. The resulting solution was transferred into a syringe fitted with a 0.84 mm internal diameter needle and electrospun using a HOLMARC HO-NFES-040 unit attached to a HMPSKV30 power supply (0–30 kV, 0.5 mA). Electrospinning was performed under optimized parameters: 11.5 kV voltage, 12.3 cm needle-to-collector distance, and a 0.4 mL/h flow rate. Nanofiber mats were produced over 6 to 8 hours at room temperature [8, 38, 39].

2.6. Physicochemical characterization

2.6.1. UV–visible spectroscopy

To confirm nanoparticle formation and analyze optical properties, UV–Vis spectra were recorded using a VIS SPEC V-730 spectrophotometer across the 200–800 nm range with deionized water as the blank. Distinct absorbance peaks suggested surface plasmon resonance and verified nanoparticle inclusion in the nanofibers [40].

2.6.2. FTIR spectroscopy analysis

FTIR spectra were obtained using a PerkinElmer Spectrum Two with ATR mode to identify chemical bonds and molecular interactions. Spectral data were collected over a 4000–400 cm^{-1} range with 64 scans at 4 cm^{-1} resolution. Functional groups like hydroxyl, carbonyl, amide, and Cu–O bonds were examined to assess interactions within the scaffold matrix [41].

2.6.3. XRD analysis

XRD analysis of CuO NPs and fabricated scaffolds was performed using a Bruker D8 Advance with CuKα radiation ($\lambda = 1.5406$ Å), operating at 40 kV and 40 mA. Scans were recorded from $2\theta = 5°$ to 90° with a step size of 0.029649°. Monoclinic CuO peaks were matched, and any shifts or new patterns were interpreted for matrix interaction [42].

2.6.4. SEM analysis

Surface morphology and nanofiber distribution were analyzed via SEM (JEOL JSM-IT800 NANO). Samples were gold-coated before imaging to minimize charging. The micrographs offered structural insights, including fiber diameter, nanoparticle embedding, and uniformity of the scaffold [43].

2.6.5. TGA

Thermal properties were determined using the PerkinElmer TGA 8000. Around 5 mg of each sample was heated from room temperature to 550°C at a rate of 15°C/min under a nitrogen atmosphere. Thermograms illustrated moisture loss, degradation events, and thermal robustness of the samples [44].

2.6.6. Zeta potential and DLS

The Malvern Zetasizer Ultra was employed to measure DLS and zeta potential for the CuO NPs. These measurements helped determine particle size distribution and surface charge, thereby providing insights into colloidal stability in solution [45].

All raw and processed data have been publicly archived in the Mendeley Data repository (DOI: 10.17632/vf8822rd8j.2) for open access and reproducibility.

2.7. Wound healing (scratch) assay

To assess wound healing potential, the scratch assay was conducted using HaCaT keratinocytes treated with algal extract, CuO NPs, and starch/PVA/CuO-NPs nanoscaffolds. Cells were seeded at 2×10^5 cells/well in 12-well

plates using DMEM with 10% FBS and 1% penicillin-streptomycin, then incubated at 37 °C with 5% CO_2 until confluent. A sterile 200 µL pipette tip created a uniform wound across each well. After washing with PBS, cells were treated with test samples at 6.25, 12.5, 25, 50, and 100 µg/mL in serum-free DMEM. Untreated wells served as controls. Wound closure progression was observed at 0, 24, and 48 hours under a phase-contrast microscope. ImageJ software was used to calculate wound closure percentage for each sample and dosage to assess healing performance [46].

2.8. Statistical analysis

All experimental results were analyzed statistically using SPSS v25.0 and GraphPad Prism v9.0. Data are expressed as mean ± standard deviation from triplicate tests. Differences among groups were determined by one-way ANOVA followed by Tukey's or Dunnett's post hoc test. A significance level of $p < 0.05$ was adopted. Pearson correlation tested inter-variable associations. Data normality was verified via the Shapiro–Wilk test, and log transformation was applied if normality assumptions failed. A 95% confidence level was maintained for all interpretations [47].

3. RESULTS

3.1. UV–visible spectroscopy

The UV–Visible absorption spectra (Fig. 1) obtained from the aqueous extract of *S. wightii* and the green-synthesized CuO NPs revealed clear indicators of successful nanoparticle formation and their optical features. The algal extract displayed a sharp peak at 346 nm, which is typically associated with polyphenolic and flavonoid constituents. These phytochemicals are assumed to function simultaneously as both reducing and capping agents in the nanoparticle synthesis process. In contrast, the CuO NPs exhibited a unique absorption peak at 292 nm, characteristic of surface plasmon resonance (SPR), confirming nanoparticle formation. Furthermore, a wide absorption range between 400 and 800 nm was evident, possibly due to particle clustering or matrix interactions. The spectroscopic analysis was conducted using a VIS SPEC V-730 spectrophotometer spanning 200–800 nm, with deionized water used as the blank. The absence of extraneous spectral bands indicates the purity of the synthesized particles. The identified SPR signatures are consistent with known optical responses of metal oxide nanoparticles, validating the use of *S. wightii* extract as a suitable medium for green nanoparticle synthesis.

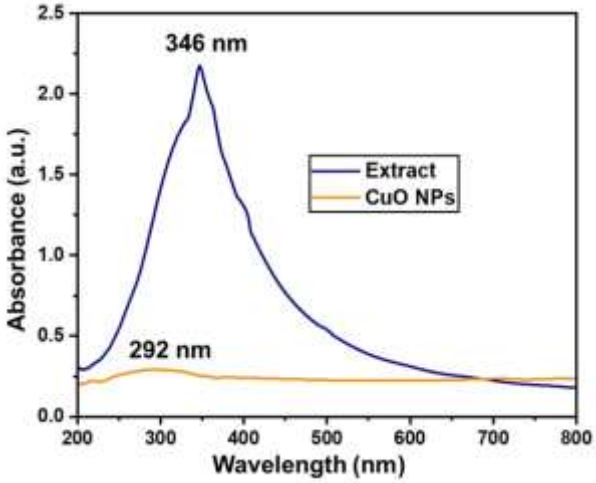

Fig. 1. UV–Visible spectral profiles of algal extract and CuO NPs.

3.2. FTIR spectroscopy analysis

FTIR spectroscopy (Fig. 2) was used to analyze the molecular functional groups present in both the CuO NPs and the starch/PVA nanoscaffolds. The spectra were recorded using the PerkinElmer Spectrum Two in ATR mode, scanning from 4000 to 400 cm^{-1} at a resolution of 4 cm^{-1} with 64 accumulations. The FTIR spectrum of the CuO NPs exhibited several characteristic bands denoting different organic and inorganic functional groups involved in stabilization and metal-oxygen bonding. The nanoscaffold spectrum displayed significant peaks at 3298.42 cm^{-1} (hydroxyl and amine stretching), 2924.17 cm^{-1} (aliphatic C–H stretching), 1710.48 cm^{-1} (carbonyl C=O stretching), 1426.82 cm^{-1} (symmetric COO^- stretching or CH_2 bending), and 1097.57 cm^{-1} (C–O–C or siloxane vibrations). Minor bands observed at 1329.64, 919.55, and 843.63 cm^{-1} were assigned to C–N bonds, phosphoester linkages, or Cu–O stretches. The noticeable shifts and broadening of several peaks, alongside the absence of contamination signals, point toward substantial intermolecular interactions, possibly via hydrogen bonding or electrostatic attractions, between the nanoparticles and the polymer components. These spectral profiles confirm successful nanoparticle integration into the matrix and hint at potential alterations in scaffold functionality due to these molecular interactions.

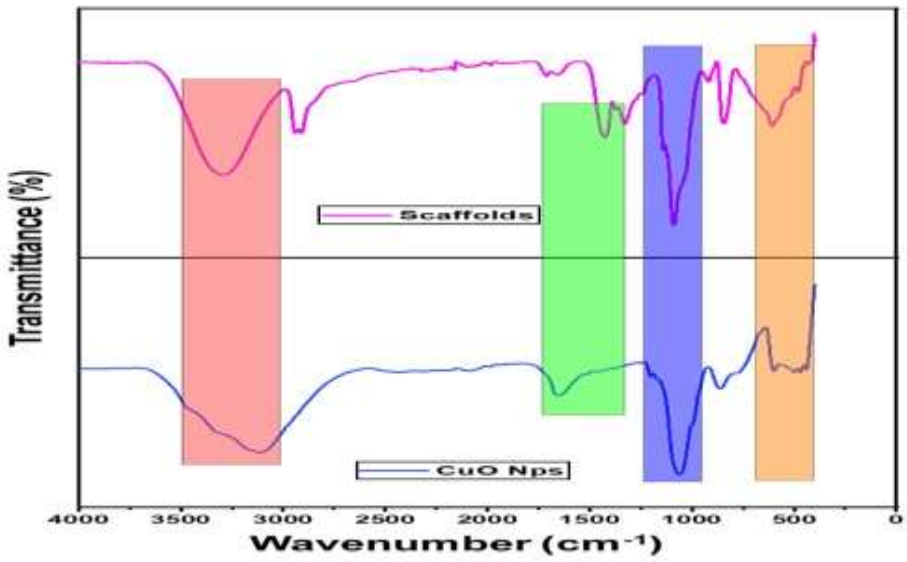

Fig. 2. FTIR spectra of CuO NPs and their incorporation into nanoscaffolds.

3.3. XRD analysis

XRD studies (Fig. 3) were performed to assess the crystalline nature of the synthesized CuO NPs and the electrospun starch/PVA scaffolds using a Bruker D8 Advance instrument with CuKα radiation (λ = 1.5406 Å), operating at 40 kV and 40 mA. The diffraction patterns were scanned over a 2θ range of 5° to 90°, using a 0.029649° increment. The CuO NPs exhibited 32 distinct diffraction peaks, notably at 16.386°, 22.406°, 24.107°, 31.894°, 32.745°, 38.307°, and 48.057°, corresponding to interplanar spacings of 5.405, 3.965, 3.689, 2.804, 2.733, 2.348, and 1.892 Å, respectively. These peaks confirmed the monoclinic crystal structure of CuO (JCPDS 05-0661). Strong intensity peaks at 22.406° and 24.107°, with relative intensities of 80.2% and 100%, supported the highly crystalline nature of the nanoparticles. The broad nature of peaks indicated the nanoscale crystallite sizes. The scaffold's diffraction pattern showed semi-crystallinity with 45.3% crystalline and 54.7% amorphous content. Peaks at 29.372°, 38.502°, and 44.687° were linked to embedded CuO, though with minor shifts and attenuated intensities, reflecting the effect of polymer embedding. The full width at half maximum (FWHM) ranged from 0.130°–0.341° for the scaffold and 0.115°–0.580° for the nanoparticles. No foreign peaks were detected, confirming purity. Peak broadening in scaffolds suggests decreased crystallinity, influenced by the amorphous polymer matrix.

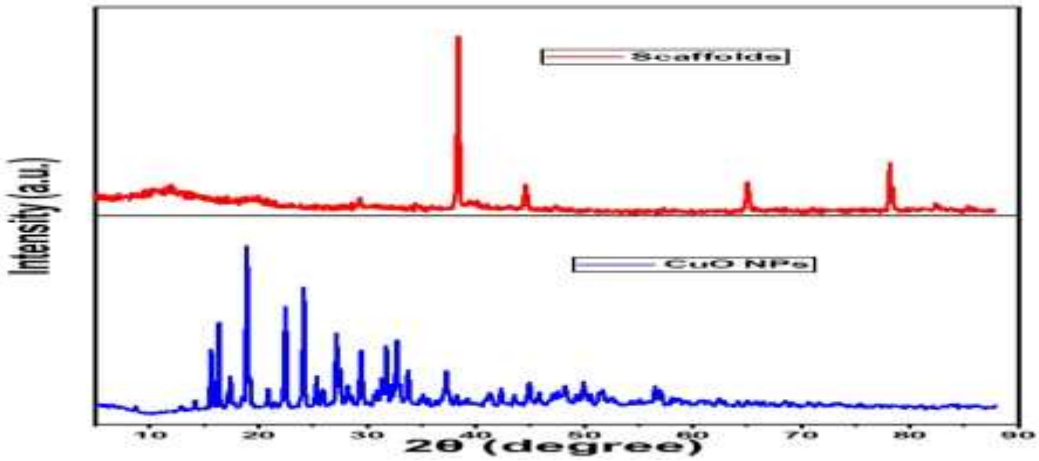

Fig. 3. XRD patterns of synthesized CuO NPs and CuO-loaded scaffolds.

3.4. SEM analysis

SEM images (Fig. 4) were captured using the JEOL JSM-IT800 NANO microscope to investigate the morphology of both CuO NPs and the nanofibrous scaffolds. Samples were coated with a thin layer of gold prior to analysis to reduce charging effects. The CuO NPs appeared spherical and uniformly distributed, indicating successful synthesis without notable clumping. The starch/PVA electrospun fibers formed a dense, porous, and continuous fibrous mesh. The CuO NPs were well-embedded along the fiber surfaces, exhibiting no aggregation, which is essential for homogeneity and functionality. The absence of beads and the consistent diameter across fibers suggested optimal electrospinning conditions. Such uniform morphology enhances cell attachment, nutrient diffusion, and mechanical integrity—important attributes for biomedical applications. The homogenous

dispersion of CuO NPs further augments potential antimicrobial and catalytic properties, making the scaffold suitable for tissue regeneration and therapeutic delivery.

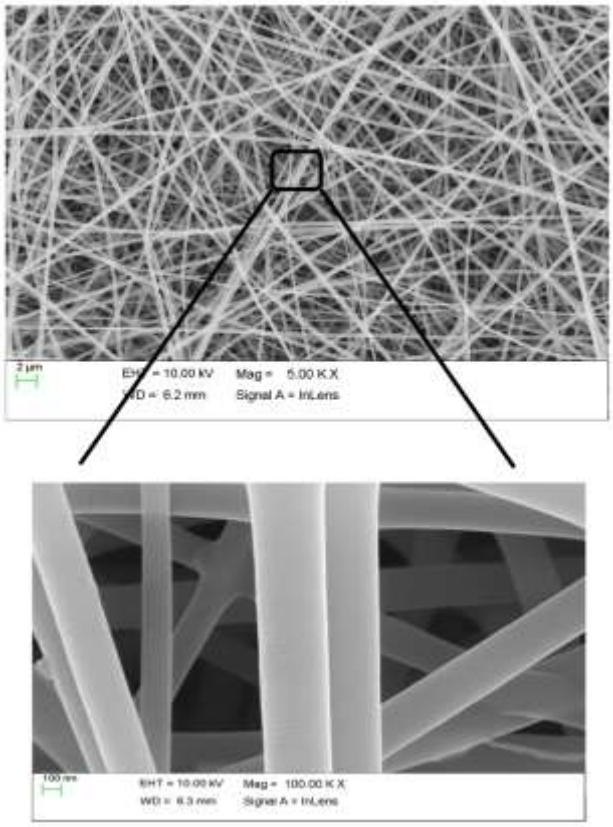

Fig. 4. SEM analysis of synthesized CuO NPs and CuO-loaded scaffolds.

3.5. TGA

TGA (Fig. 5) was carried out to understand the thermal behavior of the starch/PVA scaffolds using the PerkinElmer TGA 8000. A 5.518 mg sample was subjected to a heat ramp from ambient temperature to 550°C at 15°C/min in a nitrogen environment. The thermal decomposition exhibited three distinct stages. The first weight loss occurred below 150°C due to water evaporation. The main decomposition phase started at 220.95°C and concluded around 382.16°C, peaking at 322.94°C, corresponding to the degradation of the polymer matrix (starch and PVA), particularly hydroxyl and glycosidic groups. This stage led to a 37.126% mass loss. Beyond 382.16°C, the mass remained stable, indicating the formation of a thermally stable residue, possibly comprising CuO. The analysis revealed that the scaffolds possess thermal resistance up to 220°C, allowing for heat-based sterilization. The presence of CuO may contribute marginally to enhanced thermal stability, though its detailed influence requires further investigation through comparative analyses.

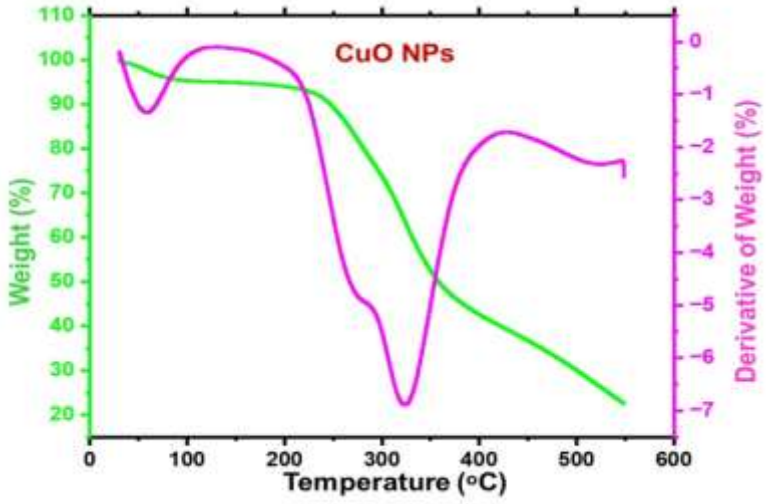

Fig. 5. Thermal degradation behavior of CuO-incorporated nanoscaffolds.

3.6. Zeta potential and particle size

DLS and zeta potential measurements of the CuO NPs were undertaken using a Malvern Zetasizer Ultra to evaluate their colloidal stability and size in dispersion. The hydrodynamic diameter obtained via DLS averaged 146.1 nm (Fig. 6), indicating a narrow particle size distribution and monodispersity. Zeta potential analysis revealed a significantly negative surface charge of −120 mV (Fig. 7), denoting excellent electrostatic stability that minimizes aggregation. Generally, zeta potentials above ±30 mV reflect strong particle repulsion, suggesting a stable colloidal system suitable for biomedical and catalytic systems. The high magnitude of surface charge and uniform particle size indicate effective bio-capping and stabilization via algal constituents during green synthesis. These traits affirm the nanoparticles' stability in aqueous environments and support their compatibility for long-term storage and *in vivo* applications.

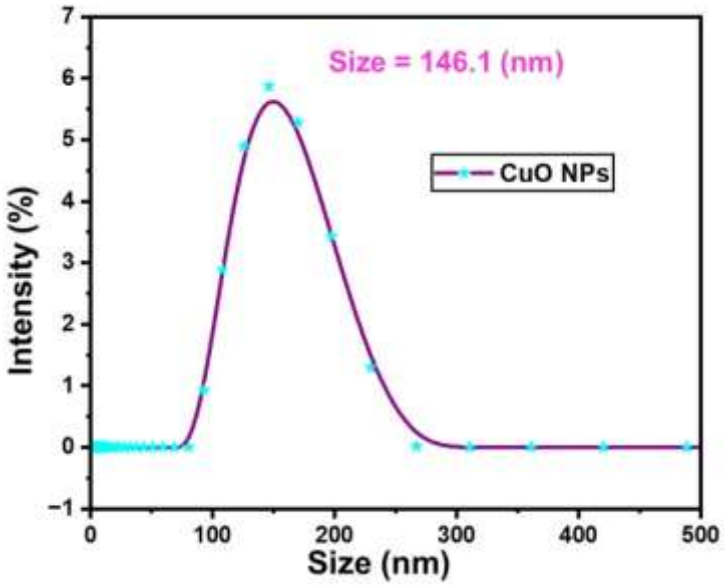

Fig. 6. DLS particles size analysis of CuO NPs

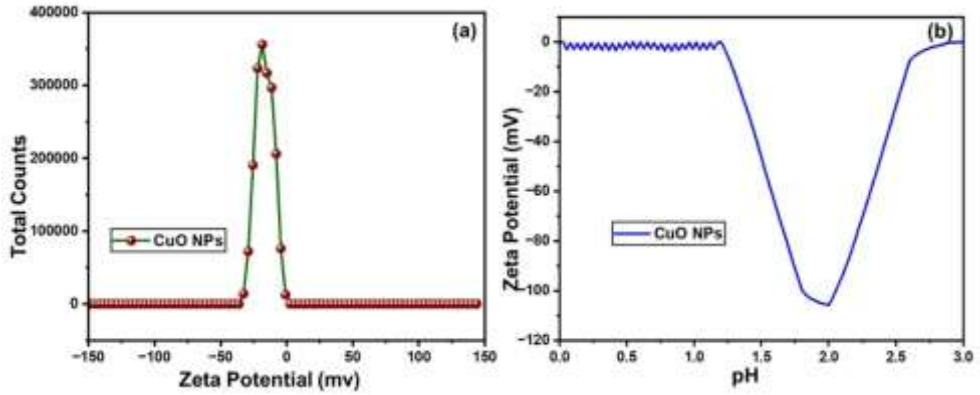

Fig. 7. Zeta-potential analysis of CuO NPs

3.7. Wound healing (scratch) assay

After 48 hours of treatment, the wound healing assay (Fig. 8) demonstrated significant differences in the migratory behavior of HaCaT keratinocyte cells exposed to algal extract, CuO NPs, and starch/PVA/CuO-NPs nanoscaffolds. The percentage of wound closure was quantified to evaluate the efficacy of each treatment at concentrations of 6.25, 12.5, 25, 50, and 100 µg/mL.

The algal extract exhibited a concentration-dependent increase in wound closure, with rates of 33.62%, 40.62%, 51.62%, 61.62%, and 70.62% at the respective concentrations. These results indicate that the algal extract promoted moderate cell migration, with higher concentrations enhancing the healing process more effectively.

In contrast, CuO NPs demonstrated a more pronounced wound healing effect, achieving closure rates of 41.62%, 47.62%, 63.62%, 65.62%, and 84.62% across the tested concentrations. The superior performance of CuO NPs suggests their potential in accelerating keratinocyte migration, particularly at higher doses.

The starch/PVA/CuO-NPs nanoscaffolds displayed the highest wound closure efficiency among the tested samples, with rates of 48.62%, 63.62%, 74.62%, 80.62%, and 96.62%. This remarkable performance highlights the synergistic effect of the nanoscaffold’s composite structure, which likely provided an optimal microenvironment for cell migration and proliferation.

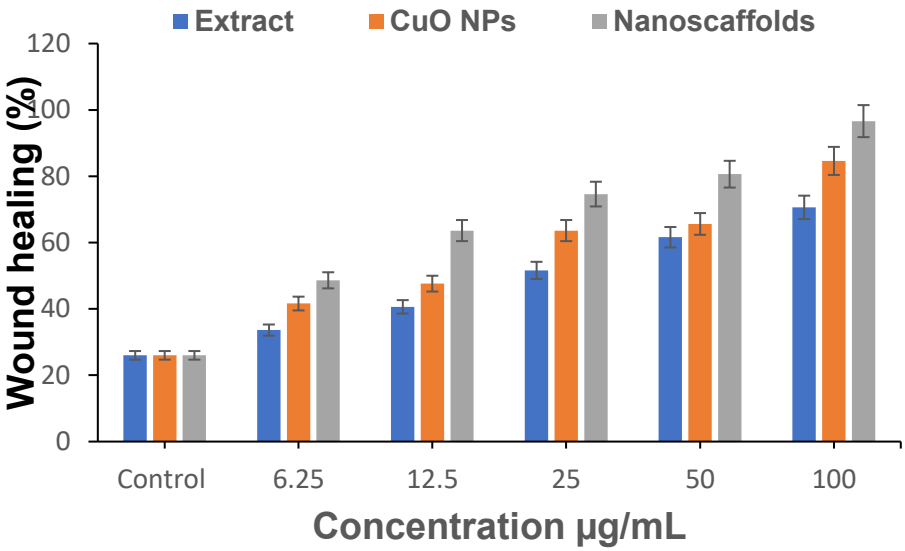

Fig. 8. Wound healing activity analysis of algal extract, CuO-NPs and starch/PVA/CuO-NPs nanoscaffolds

The nanoscaffolds consistently outperformed both the algal extract and CuO NPs at all concentrations, indicating their superior wound healing potential. While the algal extract showed moderate activity, CuO NPs exhibited intermediate efficacy, suggesting that the incorporation of CuO NPs into the nanoscaffold structure significantly enhanced their biological activity. These findings underscore the potential of starch/PVA/CuO-NPs nanoscaffolds as a promising therapeutic agent for wound healing applications.

The assay confirmed that all three treatments facilitated wound closure in a dose-dependent manner, with the nanoscaffolds emerging as the most effective. Further studies could explore the underlying mechanisms, such as cell proliferation and extracellular matrix remodeling, to fully elucidate their therapeutic potential.

4. DISCUSSION

The *in vitro* wound healing analysis of starch/PVA electrospun nanoscaffolds incorporated with ultrasonic-assisted green synthesized CuO NPs using *S. wightii* extract demonstrated compelling evidence of their therapeutic efficacy. The comprehensive assessment included optical, structural, morphological, thermal, and biological evaluations, each contributing unique insights into the scaffold's potential for wound care applications.

UV–Visible Spectroscopy provided the initial confirmation of successful nanoparticle formation. The algal extract displayed a strong absorbance peak at 346 nm, a signature commonly linked to the presence of flavonoids and polyphenolic compounds, which play key roles in reducing and stabilizing metal ions during biosynthesis. Upon nanoparticle formation, a distinct peak at 292 nm emerged, confirming the presence of surface plasmon resonance—a characteristic optical property of metallic nanoparticles. The presence of a broader absorbance from 400–800 nm likely points to interparticle interactions or slight agglomeration, which can occur in aqueous suspensions. Notably, the absence of additional peaks suggested high nanoparticle purity, and the spectral signatures matched known features of CuO NPs. These findings substantiate the dual functionality of *S. wightii* extract in facilitating and stabilizing nanoparticle synthesis via a green approach [48-53].

FTIR Spectroscopy Analysis revealed the molecular interactions and functional groups involved in nanoparticle formation and scaffold integration. The CuO NPs exhibited various absorption bands indicative of metal-oxygen and biomolecular interactions. Meanwhile, the electrospun scaffold spectrum presented characteristic peaks for hydroxyl, amine, carbonyl, aliphatic, and ether groups, which are consistent with the constituents of starch and PVA. Additionally, absorption bands associated with Cu–O bonding confirmed the successful embedding of nanoparticles within the polymeric matrix. Shifts in peak positions and band broadening were observed, suggesting intermolecular interactions such as hydrogen bonding or electrostatic forces between the CuO NPs and the scaffold components. This molecular compatibility ensures structural integrity and could influence the scaffold's bioactivity [54-59].

XRD Analysis provided insights into the crystallinity and phase composition of the CuO NPs and the electrospun scaffold. The diffraction pattern of the nanoparticles aligned with the monoclinic tenorite phase of CuO, as per JCPDS reference 05-0661. High-intensity peaks and their broadening confirmed both crystallinity and nanoscale dimensions. In contrast, the starch/PVA/CuO scaffold exhibited a semi-crystalline nature with identifiable peaks corresponding to CuO. However, peak intensities were reduced, and slight positional shifts were recorded, which likely reflect the interaction of CuO NPs with the amorphous polymeric environment. The lack of extraneous peaks confirmed the purity of the materials. These structural characteristics suggest that the nanoscaffold maintains a balance between crystallinity and flexibility, essential for biomedical use [60-66].

SEM Imaging further validated the morphological features of both CuO NPs and the nanoscaffolds. The CuO NPs were found to be spherical and well-dispersed, indicating successful synthesis without significant aggregation.

The electrospun scaffolds exhibited a fibrous, porous structure with uniform fiber diameter and absence of bead formation. Importantly, CuO NPs were evenly distributed across the fibers without clumping, reflecting homogeneity—a critical aspect for wound dressing applications. This uniform distribution is vital not only for mechanical consistency but also for ensuring even antimicrobial activity across the scaffold. The porous architecture also facilitates gas exchange and cell migration, enhancing the scaffold's wound healing capabilities [67-71].

TGA explored the thermal stability of the scaffolds. The scaffold underwent three distinct stages of degradation: moisture loss below 150°C, major polymer decomposition between 220.95°C and 382.16°C, and a final stable residue beyond 382.16°C, likely composed of CuO. The onset of major degradation at above 220°C implies the scaffold can withstand typical sterilization processes, making it suitable for biomedical usage. The thermal behavior mirrored that of standard starch/PVA matrices, but the presence of CuO NPs potentially contributed to slight improvements in thermal resistance [72-77].

Zeta Potential and Particle Size Analysis revealed important colloidal properties. The CuO NPs demonstrated a hydrodynamic diameter of approximately 146.1 nm, indicating their nanoscale nature and narrow size distribution. The zeta potential measured −120 mV, suggesting exceptional colloidal stability due to strong electrostatic repulsion. Such a high negative charge prevents particle aggregation in aqueous systems, ensuring long-term dispersion and functional reliability. These parameters are crucial for ensuring the NPs maintain their efficacy and stability in physiological conditions [78].

The Wound Healing (Scratch) Assay offered the most direct evidence of the biomedical efficacy of the formulated nanoscaffolds. The assay revealed that all tested materials (algal extract, CuO NPs, and nanoscaffolds) exhibited a dose-dependent enhancement in wound closure after 48 hours. The algal extract alone promoted moderate cell migration, with closure rates ranging from 33.62% to 70.62%. CuO NPs significantly improved this performance, achieving up to 84.62% closure. However, the starch/PVA/CuO-NPs nanoscaffold outperformed both, demonstrating remarkable closure rates up to 96.62%. This superior effect is likely attributable to the synergistic interplay between the bioactive nanoparticles and the scaffold matrix, which provides a conducive environment for cell proliferation, migration, and tissue regeneration [79, 80].

The integration of green-synthesized CuO NPs from *S. wightii* into starch/PVA electrospun scaffolds results in a multifunctional wound healing platform. The composite scaffold exhibits favorable physicochemical properties, including high thermal stability, excellent nanoparticle distribution, and desirable molecular interactions. Most importantly, it demonstrates enhanced wound healing capabilities *in vitro*, significantly outperforming individual components. These findings support the potential application of such nanoscaffolds as advanced wound dressings, warranting further exploration through *in vivo* models and clinical studies.

5. CONCLUSION

This study successfully demonstrated the green synthesis of CuO NPs using *S. wightii* extract and their incorporation into starch/PVA electrospun nanoscaffolds for enhanced wound healing applications. Comprehensive characterization through UV-Vis, FTIR, XRD, SEM, TGA, and DLS confirmed the formation of stable, crystalline CuO NPs with uniform dispersion in the nanofibrous scaffold matrix. The nanoscaffolds exhibited excellent thermal stability, porous morphology, and colloidal properties, making them suitable for biomedical use. *In vitro* wound healing assays revealed that the starch/PVA/CuO-NPs nanoscaffolds significantly outperformed both the algal extract and standalone CuO NPs, achieving up to 96.62% wound closure at 100 µg/mL. This superior performance is attributed to the synergistic effects of the composite structure, which promotes cell migration and proliferation. The results highlight the potential of these nanoscaffolds as an advanced wound dressing material, combining the bioactive properties of CuO NPs with the structural advantages of biopolymers. Future research should focus on *in vivo* studies to validate biocompatibility and mechanistic insights into cellular interactions. This work paves the way for sustainable, algae-based nanotherapeutics in regenerative medicine.

Ethical Declaration: Not Applicable

Data Availability Statement: The full dataset of physiochemical characterization associated with this work is published in Mendeley Data [Dataset] Eco-conscious biomaterial design: Analytical insights into starch nanoscaffolds with green-engineered copper oxide nanoparticles using marine Sargassum wightii extract (DOI: 10.17632/vf8822rd8j.1). Disclosure: The material characterization data and figures (e.g., UV, SEM, FTIR, XRD, TGA, Zeta Potential and particle sizer) presented here were generated from a common dataset and are being reused across multiple related studies on nanomaterials. All biological analyses and conclusions are original to each manuscript.

Conflicts of Interest: The authors declare no conflicts of interest.

REFERENCES

[1] Xi J, Wang T, Xian P, Liu X, Du M, Yang H, Palanisamy CP, Lin W, Long Q. Proteomic insights uncover enhanced neurotherapeutic potential in conditioned mesenchymal stem cell-derived extracellular vesicles. Extracellular Vesicle. 2024; 3: 100037.

[2] Pei J, Natarajan PM, Umapathy VR, Swamikannu B, Sivaraman NM, Krishnasamy L, Palanisamy CP. Advancements in the synthesis and functionalization of zinc oxide-based nanomaterials for enhanced oral cancer therapy. Molecules. 2024; 29(11): 2706.

[3] Gatasheh MK, Natarajan SR, Krishnamoorthy R, Alsulami TS, Rajagopal P, Palanisamy CP, Veeraraghavan VP, Jayaraman S. Molecular analysis to identify novel potential biomarkers as drug targets in colorectal cancer therapy: an integrated bioinformatics analysis. Molecular and Cellular Oncology. 2024; 11(1): 2326699.

[4] Pei J, Yan Y, Jayaraman S, Rajagopal P, Natarajan PM, Umapathy VR, Gopathy S, Roy JR, Sadagopan CS, Thalamati D, Palanisamy CP, Mironescu M. A review on advancements in the application of starch-based nanomaterials in biomedicine: Precision drug delivery and cancer therapy. International Journal of Biological Macromolecules. 2024; 130746.

[5] Pei JJ, Yan Y, Palanisamy CP, Jayaraman S, Natarajan PM, Umapathy VR, Gopathy S, Roy JR, Sadagopan JC, Thalamati D, Mironescu M. Materials-based drug delivery approaches: Recent advances and future perspectives. Green Processing and Synthesis. 2024; 13: 20230094.

[6] Pei JJ, Deng W, Liu Y, Guo Y, Chen J, Abdu H, Khan MR, Palanisamy CP, El-Aty AM. A Comprehensive Review of Cornus officinalis: Health Benefits, Phytochemistry, and Pharmacological Effects for Functional Drug and Food Development. Frontiers in Nutrition. 2023; 10: 1309963.

[7] Alugoju P, Palanisamy CP, Anthikapalli NVA, Jayaraman S, Prasanskulab A, Chuchawankul S, Dyavaiah M, Tencomnao T. Exploring the anti-aging potential of natural products and plant extracts in budding yeast Saccharomyces cerevisiae: A review. F1000Research. 2023; 12: 1265.

[8] Lavanya M, Krishnamoorthy R, Alshuniaber MA, Manoharadas S, Palanisamy CP, Veeraraghavan VP, Jayaraman S, Rajagopal P, Padmini R. Formulation, characterization and evaluation of gelatin-syringic acid/zinc oxide nanocomposite for its effective anticancer, antioxidant and anti-inflammatory activities. Journal of King Saud University-Science. 2023; 35: 102909.

[9] Palanisamy CP, Poompradub S, Sansanaphongpricha K, Jayaraman S, Subramani K, Sonsudin F. Biosynthesis of silver nanoparticles (AgNPs) using ethanolic extract of Nigella sativa (L.) seeds promotes wound healing via PDGF and VEGF signalling pathways activation. Biocatalysis and Agricultural Biotechnology. 2023; 54: 102970.

[10] Prasad M, Jayaraman S, Natarajan SR, Veeraraghavan VP, Krishnamoorthy R, Gatasheh MK, Palanisamy CP, Elrobh M. Piperine modulates IR/Akt/GLUT4 pathways to mitigate insulin resistance: Evidence from animal and computational studies. International Journal of Biological Macromolecules. 2023; 253: 127242.

[11] Palanisamy CP, Pei JJ, Phaniendra A, Venkata AAN, Jayaraman S, Veeraragahavan VP, Sridevi G, Roy JR, Janaki CS, Thalamati D, Mironescu M, Luo Q, Chai Y, Long Q. New Strategy of Neurodegenerative Disease Treatment with Extracellular Vesicles (EVs) Derived from Mesenchymal Stem Cells (MSCs). *Theranostics*. 2023; 13(12):4138-4165. doi:10.7150/thno.83066.

[12] Palanisamy CP, Phaniendra A, Jayaraman S, Poompradub S. *Nigella sativa* L. seed extracts promotes wound healing progress by activating VEGF and PDGF signalling pathways: *An in vitro* and *in silico* study. *F1000 Research*. 2023; 12: 436.

[13] Pei JJ, Palanisamy CP, Phaniendra A, Venkata AAN, Natarajan PM, Umapathy VR, Swamikannu B, Jayaraman S, Rajagopal P, Poompradub S. A comprehensive review on bio-based materials for chronic diabetic wounds. *Molecules*. 2022; 28(2), 604.

[14] Palanisamy CP, Cui B, Zhang H, Gunasekaran VP, Ariyo A, Jayaraman S, Veeraraghavan V, Rajagopal P. A critical review on starch-based electrospun nanofibrous scaffolds for wound healing application. International Journal of Biological Macromolecules. 2022; 222 (Part: B): 1852-1860.

[15] Monisha P, Ponnulakshmi R, Nalini D, Vishnu P V, Palanisamy CP, Cui B, Shankargouda P, Selvaraj J. A comprehensive review on high fat diet-induced diabetes mellitus: An epigenetic view. The Journal of Nutritional Biochemistry. 2022; 2022: 109037.

[16] Monisha P, Selvaraj J, Mohamed AE, Mohamed E, Mosaab AEA, Vishnu PV, Srinivasan V, Vidhya RU, Shazia FJH, Kalaiselvi K, Durairaj S, Palanisamy CP, Surapaneni K M, Ponnulakshmi R. A Comprehensive review on therapeutic perspectives of phytosterols in insulin resistance: A mechanistic approach. Molecules. 2022; 27(5): 1595.

[17] Natarajan PM, Umapathy VR, Murali A, Swamikannu B. (2022). Computational Simulations of Identified marine-derived Natural Bioactive Compounds As Potential Inhibitors of Oral Cancer. Future Science OA. 2022; 8(3).

[18] Natarajan PM, Umapathy VR. Role of transcriptomics in the study of oral cancer. Frontiers in Oral Health. 2025; 6:1524364.

[19] Vidhyarekha U, Natarajan PM, Bhuminathan S, Sabarinathan J, Suba R, Vijayalakshmi P. Role of artificial intelligence in Oral Cancer. Advances in Public Health. 2024. 2024: 3664408.

[20] Ganesan A, Kumar NG, Natarajan PM, Gauthaman J. Automated classification of elongated styloid processes using deep learning models-an artificial intelligence diagnostics. Frontiers in Oral Health. 2025; 5: 1424840.

[21] Umapathy VR, Natarajan PM, Swamikannu B. Regenerative Strategies in Dentistry: Harnessing Stem Cells, Biomaterials and Bioactive Materials for Tissue Repair. Biomolecules. 2025; 15: 546.
[22] Natarajan PM. Dental Bioinformnatics-Current Scope and Future perspectives. Research Journal of Pharmacy and Technology. 2022;15(5):2351-6.
[23] Ganesan A, Kumar NG, Natarajan PM. Solanum trilobatum leaf extract-derived silver nanoparticles downregulate the PI3K/AKT/mTOR signaling pathway and attenuate oral squamous cell carcinoma cell proliferation. Journal of Herbmed Pharmacology. 2024; 13(2): 300-307.
[24] Perumal MKK, Renuka RR, Subbiah SK, Natarajan PM. Artificial intelligence-driven clinical decision support systems for early detection and precision therapy in oral cancer: a mini review. Frontiers in Oral Health. 2025; 6: 1592428.
[25] Ramesh E, Ganesan A, Lakshmi KC, Natarajan PM. Artificial intelligence-based diagnosis of oral leukoplakia using deep convolutional neural networks Xception and MobileNet-v2. Frontiers in Oral Health. 2025; 6: 1414524.
[26] Ganesan A, Kumar NG, Natarajan PM. Anticancer activity of silver nanoparticles synthesized from aqueous leaf extract of Solanum trilobatum (Purple fruit pea eggplant) on human oral cancer cells. Journal of Herbmed Pharmacololgy. 2024; 13(2): 260-268.
[27] Kunamalla R, Panagal M, Palanisamy CP. Biogenic synthesis and fabrication of starch/PVA/CuO electrospun nanoscaffolds from Sargassum ilicifolium (brown marine macroalgae) extract for anticancer activity on HT-29 and MCF-7 cancer cells. Biocatalysis and Agricultural Biotechnology. 2026; 72: 103923.
[28] Pei J, Govindaraj H, Sivaramakrishnan R, Kanniappan GV, Pandurangan V, Dhayalan VK, Mironescu M, Mironescu ID, Jayaraman S, Palanisamy PC. Sustainable fabrication of biopolymer-based (starch/PVA) nanoscaffolds loaded with green-synthesized CuO nanoparticles from Sargassum wightii (marine macroalgae): Cytocompatibility and antioxidant activity. Biomaterials Advances. 2026; 182: 214660.
[29] Pei J, Perumal NC, Meng P, Long Q, Palanisamy CP. Extracellular vesicle-based biosensors for Alzheimer's disease: A new frontier in precision diagnostics. Ageing Research Reviews. 2026; 113: 102904.
[30] Shree P, Sivaramakrishnan R, Kanniappan GV, Pandurangan V, Jayaraman S, Dhayalan VK, Mironescu M, Mironescu ID, Palanisamy CP. Antioxidant and biocompatible CuO-starch/PVA nanoscaffolds via ultrasonic green synthesis using Turbinaria conoides (brown marine macroalgae). Medicine in Drug Discovery. 2025; 28: 100238.
[31] Gong J, Lin J, Guan T, Pei J, Palanisamy CP, El-AtyFrom AMA. selenium tolerance to nanoplastic antagonism: Comprehensive characterization of L. casei SNUT1 and its extracellular vesicle–nanoselenium complex. Food Bioscience. 2025; 74: 107749.
[32] Poochi SP, Sundarraj R, Raju MV, Chandrasekaran MK, Ahalliya RM, Palanisamy CP, Kanniappan GV, Kondapavuluri BK, Thiruvengadam M. Harnessing Nature: Computational and Experimental Insights Into *Ipomoea obscura* Metabolites for Bladder Cancer Therapy. Chemistry and Biodiversity. 2025; 0: e00909.
[33] Dugganaboyana GK, Kannankumar MKG, Shivaramakrishna S, Raju MV, Chandrasekaran MK, Ahalliya RM, Panneerselvam N, Palanisamy CP, Kanniappan GV. Phytochemical insights, antioxidant activity and therapeutic potential of Cassia senna against prostate cancer in Wistar albino rats. Discover Applied Sciences. 2025; 7:1206.
[34] Natarajan SR, Krishnamoorthy R, Alshuniaber MA, Gatasheh MK, Rajagopal P, Veeraraghavan VP, Palanisamy CP, Jayaraman S. KDM1A Facilitates Oncogenic Potential in Colorectal Cancer Progression Through the Activation of AXIN/GSK3β/β-Catenin Signaling Pathways: Evidence From Integrated Transcriptomics and In Vitro Studies. The Journal of Gene Medicine. 2025; 27(11): e70053.
[35] Guan T, Gong J, Lin J, Palanisamy CP, Jinjin Pei J, El-Aty AMA. Machine learning-driven multimodal optimization of selenium biotransformation and flavor profiling in fermented apple–Yacon functional beverages. Innovative Food Science & Emerging Technologies. 2025; 105: 104198.
[36] Natarajan SR, Krishnamoorthy R, Alshuniaber MA, Alsulami TS, Gatasheh MK, Rajagopal P, Palanisamy CP, Govindan R, Veeraraghavan VP, Jayaraman S. ABCE1 facilitates tumour progression via aerobic glycolysis and inhibits cell death in human colorectal cancer cells through the p53 signalling pathway. Scientific Reports. 2025; 15: 24674.
[37] Huang Y, Guo H, Liu Y, Jin W, Palanisamy CP, Pei J, Oz F, El-Aty AMA. Effects of Natural Polysaccharides on the Gut Microbiota Related to Human Metabolic Health. Molecular Nutrition & Food Research. 2025; 69:e202400792.
[38] Poornima K, Meenakshi K.C, Manikandan V.R, Shankari G, Prabhu D, Rathi M.A, Palanisamy CP, Balaji R, Gopalakrishnan V.K. Exploring the anticancer potential of Jerantinine A from *Tabernaemontana coronaria* against prostate, breast, and ovarian cancers: A computational approach. *Journal of Complementary and Integrative Medicine*, 2025 22(2): 363–372.
[39] Palanisamy CP, Poompradub S, Sansanaphongpricha K, Jayaraman S, Subramani K. Faridah Sonsudin gGreen synthesis of Nigella sativa-mediated silver nanoparticles for enhanced antibacterial activity and wound healing: Mechanistic insights and biomedical applications. Environmental Nanotechnology, Monitoring & Management. 2025; 24: 101085.

[40] Surendran N, Raju MV, Chandrasekaran MK, Ahalliya RM, Palanisamy CP, Chandrasekaran G, Kanniappan GV. Physicochemical characterization of starch from Maranta arundinacea L.(arrowroot) rhizomes and its inhibition of COX-2: In vivo validation. Bioactive Carbohydrates and Dietary Fibre. 2025; 33: 100465.
[41] Kannappan P, Chandrasekaran MK, Raju MV, Gopalakrishnan S, Dhamodharan P, Ahalliya RM, Palanisamy CP, Raju B, Kanniappan GV. Exploring the anticancer potential of Jerantinine A from Tabernaemontana coronaria against prostate, breast, and ovarian cancers: a computational approach. Journal of Complementary and Integrative Medicine. 2025; 22(02): 363-372.
[42] Pei J, Kumarasamy RV, Jayaraman S, Kanniappan GV, Long Q, Palanisamy CP. Quercetin-functionalized nanomaterials: Innovative therapeutic avenues for Alzheimer's disease management. Ageing Research Reviews. 2025; 104: 102665.
[43] Jayaraman S, Prasad M, Natarajan SR, Krishnamoorthy R, Alshuniaber MA, Gatasheh MK, Veeraraghavan VP, Rajagopal P, Palanisamy CP. Molecular mechanisms underlying the effects of beta-sitosterol on TGF-β1/Nrf2/SIRT1/p53-mediated signaling in the kidney of a high-fat diet and sucrose-induced type-2 diabetic rat. Chemico-Biological Interactions. 2025; 411: 111443.
[44] Huang Y, Guo H, Liu Y, Jin W, Palanisamy CP, Pei J, Oz F, El-Aty AMA. Effects of Natural Polysaccharides on the Gut Microbiota Related to Human Metabolic Health. Molecular Nutrition & Food Research. 2025; e202400792.
[45] Prabhakaran P, Palanisamy CP, Shanmugam A, Damodharan P, Swaminathan H, Devaraj D, Ahalliya RM, Kanniappan GV. Isolation, structural characterization, and molecular docking studies on the bioactive compound from n-Hexane extract of Emilia sonchifolia (L.) DC against the pancreatic cancer target Aurora 2 Kinase. Journal of Complementary and Integrative Medicine. 2024; 22(1): 0290.
[46] Jiang H, Kumarasamy RV, Pei J, Raju K, Kanniappan GV, Palanisamy CP. Integrating engineered nanomaterials with extracellular vesicles: Advancing targeted drug delivery and biomedical applications. Frontiers in Nanotechnology. 2024; 6: 1513683.
[47] Guo H, Liu Y, Wan T, Song D, Palanisamy CP, Geng J, Pei J, Özmen S, El-Aty AMA. Toward personalized cancer management: Role of precision nutrition–diet interventions. Journal of Functional Foods. 2024; 123: 106584.
[48] Natarajan SR, Krishnamoorthy R, Alshuniaber MA, Al-Anazi KM, Farah MA, Rajagopal P, Palanisamy CP, Veeraraghavan VP, Jayaraman S. Identification of FOXM1 as a novel protein biomarker and therapeutic target for colorectal cancer progression: Evidence from immune infiltration and bioinformatic analyses. International Journal of Biological Macromolecules. 282 (Part 4): 137201.
[49] Rajendran MS, Jayaraman S, Khan JM, Jasmine S, Prabhakaran RK, Raju MV, Chandrasekaran MK, Ahalliya RM, Kannappan P, Palanisamy CP, Kanniappan GV. Investigating the colon toxicity and carcinogenic role of monosodium glutamate compared with Dimethylhydrazine in male Wistar rats: Exploring the link to childhood colon cancer risk. Journal of King Saud University - Science. 2024; 36(11): 103507.
[50] Kumarasamy RV, Natarajan P, Umapathy VR, Roy JR, Rab SO, Saeed M, Panagal M, Mironescu M, Srinivasan GP, Palanisamy CP. Clinical Applications and Therapeutic Potentials of Advanced Nanoparticles: A Comprehensive Review on Completed Human Clinical Trials. Frontiers in Nanotechnology. 2024; 6:1479993.
[51] Jin W, Pei JJ, Roy JR, Jayaraman S, Ahalliya RM, Kanniappan GV, Mironescu M, Palanisamy CP. Comprehensive review on single-cell RNA sequencing: A new frontier in Alzheimer's disease research. Ageing Research Reviews. 2024; 274: 102454.
[52] Pei J, Palanisamy CP, Jayaraman S, Natarajan PM, Umapathy VR, Roy JR, Panagal M, Jayaraman S. Curcumin-loaded polymeric nanomaterials as a novel therapeutic strategy for Alzheimer's disease: A comprehensive review. Ageing Research Reviews. 2024; 99: 102393.
[53] Pei J, Palanisamy CP, Jayaraman S, Natarajan PM, Umapathy VR, Roy JR, Thalamati D, Ahalliya RM, Kanniappan GV, Mironescu M. A comprehensive review on starch-based Sustainable Edible Films Loaded with Bioactive Components for Food Packaging. International Journal of Biological macromolecules. 2024; 274 (Part-1): 133332.
[54] Palanisamy CP, poompradub S, Sansanaphongpricha K, Subramani K, Sonsudin F. Increased expression levels of PDGF and VEGF magnify the wound healing potential facilitated by biogenic synthesis of silver nanoparticles. Nano-Structures & Nano-Objects. 2024; 39: 101236.
[55] Pei J, Palanisamy CP, Jayaraman S, Natarajan PM, Umapathy VR, Roy JR, Thalamati D, Ahalliya RM, Kanniappan GV, Mironescu M. Proteomics Profiling of Extracellular Vesicle for Identification of Potential Biomarkers in Alzheimer's Disease: A Comprehensive Review. Ageing Research Reviews. 2024; 99: 102359.
[56] Natarajan PM, Swamikannu B, Sivaraman NM, Stylin AGSQ. Prevention of Oral Cancer: A Comprehensive Guide. Journal of Pharmacy and Bioallied Sciences. 2024; 16(5): S4239-S4241.
[57] Umapathy V, Dhanavel A, Kesavan R, Natarajan PM, Bhuminathan S, Vijayalakshmi P. Anticancer Potential of the Principal Constituent of Piper nigrum, Piperine: A Comprehensive Review. Cureus. 2024; 16(2): e54425.
[58] Umapathy VR, Swamikannu B, Natarajan PM, Devi R, Nandini MS, Vimalarani, Vijayalakshmi P. In Silico Molecular Docking of Ocimum sanctum Phytochemicals: Targeting Key Biomarkers in Oral Cancer. Journal of Pharmacy and Bioallied Sciences. 2024; 16(5): S4792-S4799.

[59] Natarajan PM, Bhuminathan S, Rajan R, Bindu K, Loganathan K, Veerakumar R. The Crucial Role of Smoking Cessation in Preventing Oral Cancer. Journal of Pharmacy and Bioallied Sciences. 2024; 16(5): S4245-S4247.
[60] Swamikannu B, Umapathy VR, Natarajan PM, Nandini MS, Stylin AGSQ, Vimalarani V, Rajinikanth S. Unlocking the Therapeutic Benefits of Artemisia Annua: A Comprehensive Overview of its Medicinal Properties. Journal of Pharmacy and Bioallied Sciences. 2024; 16(5): S4248-S4253.
[61] Natarajan PM. Computational Studies on Recent Congeners of Fluoroquinolones and Nitroimidazoles for Their Use in Periodontal Therapy. Journal of Pharmacy and Bioallied Sciences. 2024; 16(5): S4731-S4740.
[62] Yadalam PK, Arumuganainar D, Natarajan PM, Ardila CM. Artificial intelligence-powered prediction of AIM-2 inflammasome sequences using transformers and graph attention networks in periodontal inflammation. Scientific Reports. 2025; 15: 8733.
[63] Yadalam PK, Chatterjee S, Natarajan PM, Ardila CM. Comparison of light gradient boosting and logistic r egression for interactomic hub genes in Porphyromonas gingivalis and Fusobacterium nucleatum-induced perio dontitis with Alzheimer's disease. Frontiers in Oral Health. 2025; 6:1463458.
[64] Natarajan PM, Bhuminathan S, Leela B, Bindu K, Loganathan K, Ramachandran V. Smoking and its Role in Oral Cancer. Journal of Pharmacy and Bioallied Sciences 16(5): S4242-S4244.
[65] Yadalam PK, Natarajan PM, Ardila CM. Variational graph autoencoder for reconstructed transcriptomic data associated with NLRP3 mediated pyroptosis in periodontitis. Scientific Reports. 2025; 15: 1962.
[66] Pei JJ, Perumal NC, Meng P, Long Q, Palanisamy CP. AI-assisted FTIR spectroscopic profiling of exosomes: Emerging frontiers in early detection of Alzheimer's disease. Ageing Research Reviews. 2026; 103311.
[67] Raja FSD, Abraham L, Rangasamy K, Saikia K, Rathankumar AK, Mironescu M, Mironescu I, Palanisamy CP, Kanniappan GV. Next-Generation Microbiome Therapeutics: Psychobiotics and Fecal Microbiota Transplants (FMT) for Mental Health Treatment. Frontiers in Cellular and Infection Microbiology. 2026; 16: 1719357.
[68] Subramani K, Srinivasan S, Shanmugam P, Palanisamy CP, Sonsudin F, Poompradub S. Sustainable phytochemical mediated-ZnO nanoparticles derived from Crescentia cujete for toxicological evaluation and multifunctional environmental applications. Environmental Nanotechnology, Monitoring & Management. 2026; 26: 101180.
[69] Kunamalla RP, Panagal M, Palanisamy CP. Green-engineered multiscale starch/PVA nanofibrous scaffolds embedded with CuO nanoparticles from Sargassum ilicifolium for potent antimicrobial performance. Genetics and Molecular Research. 2026; 25(13s): 1-9.
[70] Dharmaprakash S, Gunasekaran VP, Sivaramakrishnan R, Kanniappan GV, Jayaraman S, Mironescu M, Rajabathar JR, Mironescu ID, Palanisamy CP. Marine macroalgae-mediated ultrasonic-assisted green synthesis of CuO nanoparticles embedded in starch/PVA electrospun nanoscaffolds for in vitro α-amylase and α-glucosidase inhibitory activity. Scientific Reports. 2026; 16: 26243.
[71] Surendran N, Chandrasekaran G, Raju MV, Chandrasekaran MK, Ahalliya RM, Palanisamy CP, Kanniappan GV, Arcot R, Alharbi NS, Thiruvengadam M. Anti-inflammatory potential of ethanolic extract of Maranta arundinacea L.: Insights from COX-2 modulation and oxidative stress analysis. South African Journal of Botany. 2026; 195: 142-151.
[72] Pei J, Senthilkumar MV, Hessini K, Subramaniyam S, Sivaramakrishnan R, Kanniappan GV, Jayaraman S, Palanisamy CP. Green fabrication of starch/PVA/CuO nanoscaffolds using marine macroalgae extract for enhanced anti-inflammatory activity. Sustainable Chemistry and Pharmacy. 2026; 51: 102397.
[73] Balasubramanian V, Loganathan L, Muthuswamy K, Viswanathan TM, Raju MV, Chandrasekaran MK, Ahalliya RM, Poorasamy J, Palanisamy CP, Dominic S, Kanniappan GV. Anticancer therapeutic efficacy of PEGylated β-galactosidase from Aspergillus terreus in DMBA-induced breast cancer: Toxicological, molecular and histopathological evaluation in Wistar rats. International Journal of Biological Macromolecules. 2026; 360: 151856.
[74] Jayaraman S, Eswaran A, Rajagopal P, Palanisamy CP, Veerakumar P, Veeraraghavan VP, Sirasanagandla SR. Neuroendocrine-associated epigenetic factors in cellular senescence: mechanisms and therapeutic implications. Biogerontology. 2026; 27(2): 64.
[75] Ponnusamy B, Rajagopal P, Palanisamy CP, Veeraraghavan VP, Jayaraman S. Mechanistic Exploration of the anticancer activity of Justicia adhatoda Plant Leaf Ethanolic Extract against Colon Cancer Cells: An in silico and in vitro Approach. Asian Pacific Journal of Cancer Prevention. 2026; 27(3): 1069-1080.
[76] Pei J, Saran VS, Sivaramakrishnan R, Kanniappan GV, Pandurangan V, Jayaraman S, Dhayalan VK, Mironescu M, Mironescu ID, Palanisamy CP. Ultrasonic-assisted, Sargassum ilicifolium (brown marine macroalgae)-mediated biogenic synthesis of CuO nanoparticles incorporated in starch/PVA electrospun nanoscaffolds: In vitro safety and antioxidant efficacy assessment. Bioorganic Chemistry. 2026; 173: 109679.
[77] Raj MAPA, Subramaniyam S, Kanniappan GV, Jayaraman S, Palanisamy CP. Sustainable fabrication of starch/PVA/CuO electrospun nanoscaffolds from Turbinaria ornata (marine macroalgae) extract: Physicochemical characterization and antidiabetic evaluation. Kuwait Journal of Science. 2026; 53(2): 100545.
[78] Pei J, Ganesh NS, Subramaniyam S, Sivaramakrishnan R, Kanniappan GV, Jayaraman S, Palanisamy CP. Sustainable fabrication of starch/PVA/CuO electrospun nanoscaffolds from Padina tetrastromatica (Brown

macroalgae) extract: Physicochemical characterization and antidiabetic assessment. Sustainable Chemistry One World. 2026; 9: 100195.
[79] Sakthiraj A, Sivaramakrishnan R, Subramaniyam S, Kanniappan GV, Pandurangan V, Jayaraman S, Dhayalan VK, Mironescu M, Mironescu ID, Palanisamy CP. Starch/PVA electrospun nanoscaffolds loaded with ultrasonic-assisted green-synthesis of CuO nanoparticles from marine macroalgae (Gracilaria corticata) extract: Cytotoxicity and antioxidant analysis. Chemical Physics Impact. 2026; 12: 101018.
[80] Raju M, Chandrasekaran MK, Loganathan L, Ahalliya RM, Mironescu M, Mironescu ID, Palanisamy CP, Kanniappan GV. Lipid remodeling and ferroptosis in phosphatidylcholine-mediated tumor–stroma crosstalk. Frontiers in Molecular Biosciences. 2026; 13: 1742305.